NATIONAL ADVISORY COMMITTEE FOR AERONAUTICS

TECHNICAL NOTE

No. 1303

A TRANSONIC PROPELLER OF TRIANGULAR PLAN FORM

By Herbert S. Ribner

Langley Memorial Aeronautical Laboratory
Langley Field, Va.

Washington

May 1947

NATIONAL ADVISORY COMMITTEE FOR AERONAUTICS

TECHNICAL NOTE NO. 1303

A TRANSONIC PROPELLER OF TRIANGULAR PLAN FORM

By Herbert S. Ribner

SUMMARY

An isosceles triangle twisted into a screw surface about its
axis is proposed as a propeller for transonic flight speeds. The
purpose is to attain the drag reduction associated with large
sweepback in a structurally practicable configuration. A mathe-
matical theory for such a propeller is presented. Calculations
taking account of wave and skin-friction drag indicate a net effi-
ciency of the order of 80 percent at Mach number 1.1. A 12-foot
propeller is estimated to be able to absorb 18,500 brake horsepower
at 840 miles per hour at sea level.

INTRODUCTION

The critical speed of a propeller can be raised by using wide
thin blade sections and by sweeping the blades forward or rearward.
High bending stresses caused by centrifugal force limit the amount
of sweep that can be used. A propeller that avoids the centrifugal
limitations is proposed, which permits designs for Mach numbers
previously considered structurally impracticable.

Theory (references 1 and 2) suggests that airfoils of triangular
plan form should exhibit a relatively good lift-drag ratio at super-
sonic speeds for which the triangle is contained well within the
conical sound wave (Mach cone) emanating from the apex. The prin-
ciple may be applied to attain efficient propulsion at transonic and
supersonic speeds by combining rotation about the axis of symmetry
with axial translation, nose forward. A twist of the plan form is
contemplated so that it forms a screw surface of high pitch. Dif-
ferent amounts of pitch for this screw surface would serve the same
function as blade angle serves for conventional propellers.

A two-view drawing of such a propeller is shown as figure 1.
The figure shows a design for a Mach number of the order of 2 chosen
to indicate the capabilities of the propeller at supersonic speed.
The practical field of application is more likely to be in the
transonic-speed range in which a blunter triangle is utilized.

SYMBOLS

M	Mach number $\left(\dfrac{\text{Flight velocity}}{\text{Speed of sound}}\right)$
$\emptyset$	velocity potential
ω	angular velocity, radians per second
n	angular velocity, revolutions per second $(\omega/2\pi)$
x, y, z	rectangular coordinates (fig. 2)
r	semiwidth of triangle at x
η	arc cos y/r; more extended significance in appendix B; propulsive efficiency
P	pressure
ρ	mass density of air
V	flight velocity
R	radius of propeller
D	diameter of propeller (base of isosceles triangle)
b	blade chord of propeller
b_0	root blade chord of propeller (height of isosceles triangle)
p	pitch of propeller
q	dynamic pressure $\left(\dfrac{1}{2}\rho V^2\right)$
t	time
J	advance-diameter ratio (V/nD)
N	normal force
Q	torque
T	thrust

Y   force parallel to y-axis

I   moment of inertia

γ acute angle between x-axis and blade section

α angle of attack

C_D drag coefficient   (Drag/qS)

S   wing area

Subscripts and superscripts:

L.E.   measured at leading edge,

T.E.   measured at trailing edge

s   due to suction

n   due to normal force ·

f   due to skin friction

p   due to pressure

i   ideal

R   resultant

wt   weighted

THEORY FOR FLAT PLAN FORM

The theory that is developed herein is derived from the theory of two-dimensional flows presented in reference 1. The present treatment for the rotating triangle, as that of reference 1 for the triangle at an angle of attack, applies to the limiting condition of very low aspect ratio. The limitations on aspect ratio are discussed in the section entitled "Aspect ratio" and in appendix A.

Reference 1 points out that the flow about a pointed airfoil of very low aspect ratio may be considered two dimensional when viewed in cross sections perpendicular to the direction of motion.

Consider a long flat triangular airfoil moving point foremost and rotating about the axis of symmetry. The flow pattern in a plane cutting the airfoil at a distance x from the nose is essentially the two-dimensional flow produced by a flat plate rotating with angular velocity ω. Figure 3 shows this flow as viewed from a reference system at rest in the undisturbed fluid for ω clockwise.

The surface velocity potential of the flow is given by (reference 3)

$$\phi = \pm \frac{1}{4}\omega r^2 \sin 2\eta$$

$$= \pm \frac{1}{2}\omega y \sqrt{r^2 - y^2} \qquad (1)$$

where $\cos \eta = \frac{y}{r}$ and the sign changes in going from the upper to the lower surface of the airfoil. From reference 1 the local-pressure difference is

$$\Delta P = 2\rho V \frac{\partial \phi}{\partial x}$$

$$= 2\rho V \frac{\partial \phi}{\partial r} \frac{dr}{dx}$$

$$= 2\rho V \frac{\partial \phi}{\partial r} \frac{R}{b_0} \qquad (2)$$

Pressure distribution.- Carrying out the differentiation indicated in equation (2) gives

$$\Delta P = \rho V \omega \left(\frac{R}{b_0}\right)^2 \frac{xy}{\sqrt{r^2 - y^2}} \qquad (3a)$$

or

$$\frac{\Delta P}{q} = 2\pi \frac{Rx}{b_0^2 J} \cot \eta \qquad (3b)$$

where J is the advance ratio V/nD. The spanwise pressure distribution (fig. 4) is thus similar at different distances x from the vertex but magnified in proportion to x.

The spanwise distribution of normal force is given by

$$\frac{dN}{dy} = \int_{L.E.}^{T.E.} \Delta F \, dx$$

which according to equation (2) is

$$\frac{dN}{dy} = 2\rho V \phi_{T.E.}$$

Inserting the value of ϕ from equation (1) results in

$$\frac{dN}{dy} = \rho V \omega y \sqrt{R^2 - y^2}$$

$$= \frac{1}{8} \rho V \omega D^2 \sin 2\eta \qquad (4)$$

This spanwise load distribution is shown in figure 5.

Torque.- The integration of $y \frac{dN}{dy} dy$ across the span gives for the torque of the untwisted propeller

$$Q = \frac{\pi}{128} \rho D^4 \omega V \qquad (5)$$

Thrust.- For the present case of a flat or untwisted airfoil, the pressure distribution normal to the surface has no forward component; therefore, any thrust must arise from suction along the leading edge. Consider the pressure distribution about a thin elliptic cylinder rotating about the axis of symmetry. (See appendix B.) There is a suction tending to separate the two halves laterally. This suction is obtained by integrating the lateral component of the pressure force from the middle of the bottom surface around the right edge to the middle of the top surface. The limiting value of this suction per unit length as the elliptic cylinder is shrunk into a flat plate is obtained as (appendix B)

$$Y = \frac{\pi}{8}\rho\omega^2 r^3 \tag{6}$$

where r is the semiwidth of the plate. The infinite negative pressure at the edges of the rotating flat plate thus gives rise to a finite suction force per unit length of edge.

The two long sides of the triangular propeller, which form the leading edges, have been considered to be sufficiently near parallel for the flow to be approximately two dimensional about any section normal to the axis of rotation. There is therefore a suction along the leading edges given by the value of Y in equation (6) wherein r is now interpreted as the local semiwidth of the airfoil at distance x from the nose. (See fig. 6.) The suction on the length of edge between y and $y + dy$ has a thrust component $Y\ dy$. The thrust per unit length of span is therefore

$$\frac{dT}{dy} = Y$$

$$= \frac{\pi}{8}\rho\omega^2 |y|^3$$

where $|y|$ has been substituted for r in equation (6) since $|y| = r$ at the edges. A graph of this thrust distribution is shown in figure 7.

The integration of dT/dy along the span gives

$$T_1 = \frac{\pi}{256}\rho\omega^2 D^4 \tag{7}$$

for the thrust of the untwisted propeller. This value, in which the profile drag is neglected, is called the ideal thrust. The ideal thrust is thus independent of forward speed so long as equation (7) is applicable. Applicability is limited to the range of small local angle of attack, or high values of V/nD.

Efficiency.- The ideal efficiency of the flat triangular propeller (that is, the efficiency with profile drag neglected) is

$$\eta_i = \frac{T_i V}{Q \omega}$$

The insertion of equations (5) and (7) gives a value of 1/2, or 50 percent. It is shown hereinafter that the addition of a suitable twist allows a peak ideal efficiency of 100 percent.

Origin of the thrust.- The wake of an ordinary propeller behaves like a twisted ribbon moving axially rearward. Backward momentum is imparted to the air within the screw threads of the ribbon. The thrust is ordinarily equated to the time rate of increase of this momentum. The untwisted triangular propeller, however, develops thrust according to the potential theory by generating a static-pressure rise outside the wake, rather than by imparting backward momentum. In this case, the wake behaves like a flat ribbon that extends from the trailing edge of the triangle and rotates rigidly with it. (See following paragraph.) This axially rotating ribbon imparts no rearward momentum, but the air disturbed by its rotation experiences a change in static pressure obtainable by Bernoulli's equation. Consider a plane $x = Constant$ that cuts the rotating wake at right angles a great distance behind the propeller. The pressure distribution is obtained and integrated over such a plane in appendix C. There results a net pressure force exactly equal to the value of thrust previously obtained.

Other relationships.- The assumption of two-dimensional flows about the triangular airfoil implies that the trailing vorticity has just the right strength to behave as a rigid extension of the widest part of the airfoil. The wake acts, therefore, like a flat ribbon of width D rotating with angular velocity ω. According to Lamb (reference 3), the kinetic energy per unit length of the wake is

$$K.E. = \frac{\pi}{256} \rho D^4 \omega^2 \tag{8}$$

With this written in the form

$$K.E. = \frac{1}{2}I\omega^2$$

the virtual moment of inertia of the flow is obtained as

$$I = \frac{\pi}{128}\rho D^4$$

The rate of increase of the total angular momentum of the wake should be a measure of the torque on the propeller. It is

$$Q = I\omega V$$

$$= \frac{\pi}{128}\rho D^4 \omega V$$

This is identical with the expression for the torque (equation (5)) obtained from a consideration of the pressure distribution over the propeller.

Again, the rate at which work is done on the fluid by the torque is

$$\text{Power input} = Q\omega$$

$$= \frac{\pi}{128}\rho D^4 \omega^2 V$$

Also, the rate at which the kinetic energy of the wake is increasing is (see equation (8))

$$\text{Wake power} = \frac{\pi}{256}\rho D^4 \omega^2 V$$

The power input minus the wake power should equal the useful power as follows:

$$\text{Thrust power} = \frac{\pi}{128}\rho D^4 \omega^2 V - \frac{\pi}{256}\rho D^4 \omega^2 V$$

$$= \frac{\pi}{256}\rho D^4 \omega^2 V$$

$$= TV$$

The thrust is therefore

$$T = \frac{\pi}{256}\rho D^4 \omega^2$$

which is in agreement with the result of equation (7) obtained from a direct consideration of the suction at the leading edge.

THEORY FOR PLAN FORM WITH TWIST

The triangular plan form of the proposed propeller may be given a helical twist. In this way, the pressure distribution normal to the surface contributes a thrustwise component. The total thrust comprises this component together with the leading-edge suction that constitutes the entire thrust for the flat propeller. It will be shown that with twist an ideal efficiency of 100 percent is approached in the limiting case of very light loading, as for a conventional propeller.

According to reference 1, the flow about a pointed airfoil of very low aspect ratio may be considered two dimensional when viewed in cross sections perpendicular to the direction of motion. This statement appears to be applicable to airfoils with small twist (high pitch) in addition to flat airfoils. In the case of a twisted airfoil, the two-dimensional-flow pattern shown in figure 3 would show a relative rotation at a different axial distance to conform to the twist of the surface. Consider a section of the propeller cut at radius y by a plane parallel to the axis of rotation. The

section makes the small angle γ with the direction of the axis. Then the angle γ is related to the pitch p by

$$\tan \gamma = \frac{2\pi y}{p} \qquad (9)$$

According to figure 8, the velocity component normal to the section is

$$\omega y \cos \gamma - V \sin \gamma$$

By virtue of equation (12) this equals

$$\omega y \cos \gamma \left(1 - \frac{J}{p/D} \right)$$

where $J \equiv \dfrac{V}{nD}$. For $\cos \eta \doteq 1,$ it is approximately

$$\omega y \left(1 - \frac{J}{p/D} \right) \qquad (10)$$

The corresponding velocity component for the flat plan form is ωy.

Torque.- According to the foregoing discussion, the slightly twisted plan form (pitch, p) rotating with angular velocity ω exhibits the same two-dimensional-flow pattern at a section x as a flat plan form rotating with angular velocity approximately $\omega \left(1 - \dfrac{J}{p/D} \right)$. The pressure distribution for the slightly twisted plan form is thus the pressure distribution for the flat plan form with $\omega \left(1 - \dfrac{J}{p/D} \right)$ in place of ω. The pressure on an element of propeller at point (x,y) of width dy and slant length $dx/\cos \gamma$ contributes to the torque an amount $y \, \Delta P \, dy \, \dfrac{dx}{\cos \gamma} \cos \gamma.$

Because the factor $\cos \gamma$ cancels, this contribution has the same form as for an untwisted plan form. Inserting $\omega\left(1 - \dfrac{J}{p/D}\right)$ for ω in equation (5) gives the total propeller torque as approximately

$$Q = \frac{\pi}{128}\rho D^4 \omega V \left(1 - \frac{J}{p/D}\right)$$

$$= \frac{1}{256}\rho \omega^2 D^5 J\left(1 - \frac{J}{p/D}\right). \tag{11}$$

This is the ideal propeller torque because profile drag has not been taken into account. It differs but little from the net propeller torque and, therefore, the subscript i is omitted.

Thrust component of leading-edge suction.- The suction Y per unit length of edge is obtained from equation (6) by replacing ω with $\omega\left(1 - \dfrac{J}{p/D}\right)$ to account for the twist, as was done for the torque. The forward component of the suction on the length of edge between y and $y + dy$ is the element of thrust. The expression $Y\, dy$ represents this element exactly for the untwisted plan form and approximately for the slightly twisted plan form. Thus

$$dT_s \doteq Y\, dy$$

$$= \frac{\pi}{8}\rho \omega^2 \left(1 - \frac{J}{p/D}\right)^2 |y|^3\, dy$$

and the integral over the span gives the suction thrust

$$T_s \doteq \frac{\pi}{256}\rho \omega^2 D^4 \left(1 - \frac{J}{p/D}\right)^2 \tag{12}$$

Thrust component of the normal force.- The forward component of the normal force on an element of propeller at point (x,y) of width dy and slant length $dx/\cos \gamma$ is

$$\Delta P \frac{dx}{\cos \gamma} dy \sin \gamma$$

which equals

$$\Delta P \, dx \, dy \frac{2\pi y}{p}$$

Integrating from the leading edge to the trailing edge gives by virtue of equation (2)

$$\frac{dT_n}{dy} = 2\rho V \phi_{T.E.} \frac{2\pi y}{p} \tag{13}$$

where ϕ is given by equation (1). Equation (13) gives the spanwise distribution of the thrust component of the normal force and is shown in figure 9. The integral over the span, with $\omega \left(1 - \dfrac{J}{p/D}\right)$ in place of ω, yields the total thrust component of the normal force

$$T_n = \frac{\pi}{128} \rho \omega^2 D^4 \frac{J}{p/D} \left(1 - \frac{J}{p/D}\right) \tag{14}$$

Net thrust.- The ideal thrust is $T_s + T_n$, which simplifies to

$$T_i = \frac{\pi}{256} \rho \omega^2 D^4 \left[1 - \left(\frac{J}{p/D}\right)^2\right] \tag{15}$$

Ideal efficiency.- The ideal efficiency of the triangular propeller with helical twist is

$$\eta_i = \frac{T_i V}{Q \omega}$$

$$= \frac{1}{2}\left(1 + \frac{J}{p/D}\right)$$

$$= \frac{1}{2}\left(1 + \frac{\text{Advance-diameter ratio}}{\text{Pitch-diameter ratio}}\right) \qquad (16)$$

where the second term in parenthesis is less than or equal to unity. If this second term exceeds unity, both thrust and torque are negative and the system acts as a windmill. Work of amount -TV is done on the system in forcing it forward through the air, and the system is capable of doing useful work -Qω against a resisting torque. The efficiency is thus expressed by the reciprocal of equation (16) in the windmill condition and cannot exceed unity in either condition.

The ideal efficiency of the system acting as a propeller approaches unity as the advance ratio increases to approach the pitch ratio. At equality the twist of the propeller exactly fits the helical path. The condition of high efficiency is, therefore, a condition of small angle of attack or light loading, just as it is for the conventional propeller.

As pointed out previously, the assumption of two-dimensional flow about the triangular airfoil implies that the trailing vorticity has just the right strength to behave as a rigid extension of the widest part of the airfoil. For a twisted triangle the wake acts therefore like a continuation of the screw surface indefinitely rearward. The twisted triangular propeller is thus a propeller of minimum induced loss of energy according to Betz's criterion (reference 4) that the wake act like a rigid screw surface in axial rotation or rearward translation.

APPLICATION OF THEORY

Failure of theory near speed of sound.- In the immediate vicinity of M = 1, the assumption of small disturbances is violated. The theory therefore fails in this region. Unpublished free-flight data show little variation of lift-curve slope and a

smooth rise of drag with Mach number through the speed of sound for
plan forms with considerable leading-edge sweepback. It is rea-
sonable, therefore, to expect no marked drop in the efficiency of
the triangular propeller at $M = 1$, although the predicted thrust
and torque may be in error.

Profile drag.- The ideal thrust and torque, for which equa-
tions have been obtained, are the values in the absence of profile
drag. The primary effect of the profile drag is a reduction in
thrust although there is an appreciable increase in torque. It is
convenient to assign the entire power wastage in profile drag to
thrust reduction. This approximation results in a simpler calcula-
tion, is conservative with respect to the thrust calculation, and
is quite accurate, although slightly conservative, in predicting
the net propulsive efficiency.

Aspect ratio.- The analysis is based on the assumption of very
small aspect ratio; that is, the triangular plan form contemplated
is an isosceles triangle of narrow vertex angle. This assumption
is adopted from reference 1, which treats the lifting triangle (wing),
and is applied herein to the axially rotating triangle (propeller).
A reasonable expectation is that the propeller theory will begin
to fail at about the same upper limiting aspect ratio as will the
wing theory. This upper limiting aspect ratio appears to be about
unity at Mach number zero, by comparison with the exact wing theory
of Krienes (see fig. 5 of reference 1) and the available low-speed
experimental data on lift-curve slope. At Mach number 1.75, the
upper limiting aspect ratio appears to be at least 0.75 according
to the comparison with experiment in figure 10 of reference 1. A
theoretical derivation in appendix A gives

$$(\text{Limiting aspect ratio})^2 = \frac{\text{Constant}}{\left|M^2 - 1\right|} \ll \frac{16}{\left|M^2 - 1\right|}$$

for any Mach number. Setting the constant equal to unity provides
an expression in agreement with the observations just made. Thus
the limiting aspect ratio for the assumption of the low-aspect-
ratio theory of reference 1 may be expressed for subsonic speeds as

$$\text{Aspect ratio} \leq \frac{1}{\sqrt{1 - M^2}}$$

and for supersonic speeds as

$$\text{Aspect ratio} \leq \frac{1}{\sqrt{M^2 - 1}}$$

The subsonic boundary will be recognized as the familiar Prandtl-Glauert factor and the supersonic boundary, as the arc-tangent of the Mach angle. A graph of these boundaries is shown in figure 10 in which it will be observed that the theory can be applied to relatively blunt triangles at transonic speeds, except very near the speed of sound where the theory is invalid.

Twist.- The vanishingly small twist assumed permitted the introduction of the approximations

$$\sin \gamma \doteq \tan \gamma \doteq \gamma$$

$$\cos \gamma \doteq 1$$

where γ is the complement of the blade angle (fig. 8). On this account, therefore, the errors caused by finite twist are no greater than would be occasioned by these trigonometric approximations. A more fundamental reason for assuming small twist was to insure applicability of the two-dimensional-flow theory of reference 1. If the pitch is not large compared with the diameter, successive "threads" of the screw surface will approach one another closely enough to spoil the approximately two-dimensional character of the flow. For both reasons, the pitch-diameter ratio should be perhaps 6 or more for good accuracy in the computation of thrust and torque. Somewhat lower values (as the value 4.37 in the example hereinafter) should still provide good estimates for the efficiency since the errors in computed thrust and torque would be expected to be comparable and in the same direction.

Tip speed.- It is tacitly assumed in the theory that the rotational tip speed is small compared with the forward speed. In practice, some deviation from this condition is necessary. This

deviation will have two effects: first, it will impair the accuracy
with which the equations predict the ideal thrust and torque; and
second, it will make a given amount of leading-edge sweepback less
effective at the blade tip than at the apex of the triangle. In
other words, the velocity component normal to the leading edge will
increase progressively from the apex to the blade tip because of
the velocity added by the rotation. Low wave drag can be maintained
with little increase in area by a slight progressive increase of
sweepback toward the blade tip. The result is a plan form inter-
mediate in shape between a triangle and the base of a flatiron.
(See fig. 11.) The analysis leading to such a plan form is given
in appendix D.

DESIGN CONSIDERATIONS

The high velocities induced at the leading edge according to
the theory will encourage both separation and formation of shock
waves. The leading edge should therefore be rounded and camber
should be used to eliminate these peak velocities. The cambered
design should maintain the same section lift coefficients that the
theory gives for the uncambered propeller (fig. 5) in order to
retain the high ideal efficiency, but the load on each section
should be redistributed from leading edge to trailing edge with the
peak eliminated. The distribution of laminar-flow sections might
be used, for example. With the load distribution thus specified,
the method of reference 5 could be used to compute the camber and
twist.

The main aim of the triangular-plan-form propeller configura-
tion is the avoidance of the excessive wave drag that penalizes
ordinary propellers at transonic speeds. On the other hand, this
reduction must not be obtained at the expense of too great an
increase in skin-friction drag or in propeller weight. Reducing
the vertex angle of the triangle reduces the wave drag but increases
the area for a given diameter without significantly increasing the
power absorption. Selection of the vertex angle is thus a com-
promise between wave drag and skin-friction drag. The skin-friction
drag may be estimated from von Kármán's skin-friction curve. The
wave drag for a double-wedge section triangular-plan-form airfoil
has been derived by Puckett in reference 2. The double-wedge sec-
tion with its sharp leading edge and abrupt change in slope is
undesirable for the reasons outlined in the preceding paragraph.
The recommended round-leading-edge sections of the same thickness
ratio would, however, be expected to give rise to comparable wave
drag.

The high-speed triangular propeller of fixed pitch will be stalled at low forward speeds because of the high pitch. The stalled rotating airfoil should experience a large pressure drag normal to the surface. A thrust would result from a forward component of this normal force because of the helical twist of the surface. A rough analysis indicates that the static thrust and torque may be of the order of half or more of the high-speed thrust and torque for the same rotational speed.

Automatic pitch control appears to be impracticablo for the complete triangular propeller; however, the triangular plan form may be cut in two near the base by a cut parallel to the base. The relatively narrow strip behind the cut will exhibit the twist and general appearance of an ordinary propeller if the sawed leading odge is rounded. The two radial halves of this strip could be mounted in an automatic-pitch-control hub. At moderate speeds the triangular part of the propeller ahead of the cut could be declutched and allowed to windmill freely; the ontire thrust would then be supplied by the section with automatic pitch control. Practicability is dependent on whether aerodynamic considerations would require the trailing edge to be too thin for such application.

OTHER APPLICATIONS

Devices that are basically airscrews or that may employ an airscrew include the propeller, windmill, fan, airspeed indicator, and air log. With conventional blade forms, difficulties are to be expected at speeds near and above the speed of sound. Robert T. Jones of the Ames Aeronáutical Laboratory has suggested that, with reference to an air log, a triangular plan form like that of figure 1 defers these difficulties to speeds well into the supersonic. Evidently, this observation is applicable to all the listed airscrew devices. The principle can also bo applied to a twisted triangle employed as a supersonic compressor (fan) or turbine (windmill) for jet propulsion.

EXAMPLE

Computations are presented in tables I and II for a propeller intended for operation at transonic forward speeds. A two-view diagram with the twist of the propeller omitted is shown in figure 11. The profile is the double-wedge (unsymmetric-diamond) section treated theoretically by Puckett (reference 2). This profile is chosen for

purposes of computation only and is not the recommended profile.
(See section entitled "Design Considerations.") In accordance with
reference 2, the line of maximum thickness is taken well forward for low
supersonic wave drag. The thickness ratio is chosen very small (0.03)
for the same reason. This thickness ratio corresponds to values of
absolute thickness comparable with those of contemporary propeller
design.

The thickness selection was made on the basis that the combined
aerodynamic and tensile stresses should not be excessive. The tip
chords were widened into swept-back extensions for the same reason
and, also, to avoid flow separation at the tips as a result of
excessive local lift coefficients. The stress considerations were
hardly elaborate enough to qualify as a stress analysis; the purpose
was merely to insure that the proportions were not unreasonable from
a structural point of view.

The diameter of the propeller (fig. 11) was taken as 12 feet
to make it comparable with diameters of present fighter airplanes.
The leading-edge sweepback of 45° was chosen as a compromise between
considerations of wave drag and skin-friction drag. The pitch-
diameter ratio p/D and advance-diameter ratio J were arrived
at by a cut-and-try process, with a view toward high power at high
efficiency without excessive tip speed and with the twist within
the bounds contemplated in the theory.

The partial modification of the plan form from a triangle
toward a flatiron shape follows the considerations developed in
appendix D. The modification compensates for the effect of the
excess of the tip velocity over the forward velocity. The degree
of flatiron curvature has been adjusted to maintain the component
velocity normal to the leading edge constant at 0.707 of the flight
speed at the design advance ratio. The computations specifying the
plan form are given in table I.

Also given in table I are values of the blade chord weighted
in such a way that multiplication of the integrated value by $\frac{1}{2}\rho V^3 C_D$,
where V is the flight velocity and C_D is the drag coefficient,
will give the amount of power consumed in overcoming profile drag.
This power divided by V is defined as the profile drag and is
subtracted from the ideal thrust to obtain the net thrust. Actually,
only part of this power loss appears as reduced thrust; the remainder
appears as increased torque. The calculation procedure is thus only
approximate.

The main steps in the calculation of the performance of this
12-foot propeller at Mach number 1.1 are itemized in table II for

sea level and 25,000 feet altitude. The results show a constant
net efficiency of 80 percent and a power absorption of about
6,200 brake horsepower at 25,000 feet and 18,500 brake horsepower
at sea level.

CONCLUDING REMARKS

1. Propellers of triangular plan form appear to be capable of
absorbing high power with good efficiency at transonic flight speeds.

2. Triangular propellers within the scope of the theory should
exhibit a rigidly behaving wake, Betz's condition for minimum induced
loss of energy.

3. The static thrust of the triangular propeller may be of the
order of half or more of the high-speed thrust.

4. The principle of the triangular propeller can be applied to
extend into the supersonic the useful range of such airscrew devices
as the air log, absolute airspeed indicator, windmill, and fan. The
principle can also be applied to a supersonic compressor (fan) or
turbine (windmill) for jet propulsion.

Langley Memorial Aeronautical Laboratory
    National Advisory Committee for Aeronautics
        Langley Field, Va., February 21, 1947

APPENDIX A

LIMITING ASPECT RATIO FOR ASSUMPTION OF LOW-

ASPECT-RATIO THEORY

For small-disturbance velocities the equation for the velocity potential in compressible flow has the linearized form

$$\left(1 - M^2\right)\frac{\partial^2 \phi}{\partial x^2} + \frac{\partial^2 \phi}{\partial y^2} + \frac{\partial^2 \phi}{\partial z^2} = 0 \tag{A1}$$

where the stream velocity is in the x-direction. The assumption of two-dimensional flows (low-aspect-ratio theory of reference 1) implies that the first term is negligible in comparison with either of the last two so that

$$\frac{\partial^2 \phi}{\partial y^2} + \frac{\partial^2 \phi}{\partial z^2} \doteq 0 \tag{A2}$$

The condition for approximately two-dimensional flows is thus

$$\left|1 - M^2\right| \frac{\partial^2 \phi}{\partial x^2} \ll \left|\frac{\partial^2 \phi}{\partial y^2}\right| \tag{A3}$$

Applying this test to the potential of a rotating line (equation (1))

$$\phi = \pm \frac{1}{2}\omega y \sqrt{r^2 - y^2}$$

$$= \pm \frac{1}{2}\omega y \sqrt{x^2\left(\frac{\text{Aspect ratio}}{4}\right)^2 - y^2}$$

gives

$$\left| 1 - M^2 \right| \left(\frac{\text{Aspect ratio}}{4} \right)^2 \frac{\omega y^3}{2\left(r^2 - y^2\right)^{3/2}} \ll \left| \frac{\omega y^3}{2\left(r^2 - y^2\right)^{3/2}} \left(3\frac{r^2}{y^2} - 2 \right) \right|$$

or

$$(\text{Aspect ratio})^2 \ll \frac{16 \left| 3\frac{r^2}{y^2} - 2 \right|}{\left| M^2 - 1 \right|} \qquad (A4)$$

Equation (A4), as equation (1), is limited in application to the surface of the triangular airfoil. From the center of the triangle to the edges, the right-hand side varies from ∞ to 16. Therefore, the criterion

$$(\text{Aspect ratio})^2 \leqq \frac{\text{Constant}}{\left| M^2 - 1 \right|} \ll \frac{16}{\left| M^2 - 1 \right|} \qquad (A5)$$

insures approximately two-dimensional flow over the entire width of the triangle.

APPENDIX B

SUCTION AT EDGES OF A ROTATING ELLIPTIC CYLINDER

Lamb (reference 3) gives the potential of the flow produced by the axial rotation of an elliptic cylinder as

$$\phi = \frac{1}{4}\omega(a + b)^2 e^{-2\xi}\sin 2\eta \qquad (B1)$$

where ω is the angular velocity (clockwise herein), a and b are the major and minor axes, respectively, and ξ and η are elliptic coordinates that are related to the rectangular coordinates by

$$\left.\begin{array}{c} y = c \cosh \xi \cos \eta \\ \\ z = c \sinh \xi \sin \eta \end{array}\right\} \qquad (B2)$$

The x-axis is the axis of the elliptic cylinder, and the relation $\xi = \xi_0$ defines the surface so that

$$a = c \cosh \xi_0$$

$$b = c \sinh \xi_0$$

(The direction assigned herein to ω differs from that implied in Lamb because of opposite sign conventions for the relation of the gradient of ϕ to the velocity.)

Equation (B1) refers to y,z axes at rest in the undisturbed fluid and instantaneously coincident with the y,z axes of the elliptic cylinder at the moment under consideration. Alternatively, ϕ may be regarded as a function of the polar coordinates r,θ relative to the fixed axes, where

$$y = r \cos \theta$$

$$z = r \sin \theta$$
\Bigg\}
\qquad (B3)

The rotation of the axes of the elliptic cylinder is taken into account by writing

$$\phi = \phi(r, \theta + \omega t)$$

The time derivative of ϕ is therefore

$$\frac{\partial \phi}{\partial t} = \omega \left(\frac{\partial \phi}{\partial \theta} \right)_r$$

The potential still refers only to disturbances relative to the fluid at rest, and its gradient is the absolute particle velocity $\bar{v}$.

Bernoulli's law states that the excess of the local pressure over the stream pressure is

$$\Delta P = -\frac{1}{2}\rho \left(2 \frac{\partial \phi}{\partial t} + v^2 \right)$$

$$= -\frac{1}{2}\rho \left[2\omega \left(\frac{\partial \phi}{\partial \theta} \right)_r + \left(\frac{\partial \phi}{\partial y} \right)_z^2 + \left(\frac{\partial \phi}{\partial z} \right)_y^2 \right]$$

This may be written more compactly

$$\Delta P = -\frac{1}{2}\rho \left(2\omega \phi_\theta + \phi_y^2 + \phi_z^2 \right) \qquad (B4)$$

where $\phi_\theta = \left(\dfrac{\partial \phi}{\partial \theta}\right)_r$, $\phi_y = \left(\dfrac{\partial \phi}{\partial y}\right)_z$, and so forth.

Implicit differentiation of ϕ leads to the relations

$$\phi_\theta = \frac{\phi_\xi\left(y_\theta z_\eta - z_\theta y_\eta\right) + \phi_\eta\left(z_\theta y_\xi - y_\theta z_\xi\right)}{J} \tag{B5}$$

$$\left.\begin{aligned} \phi_y &= \frac{\phi_\xi z_\eta - \phi_\eta z_\xi}{J} \\[2em] \phi_z &= \frac{y_\xi \phi_\eta - y_\eta \phi_\xi}{J} \end{aligned}\right\} \tag{B6}$$

where

$$J \equiv y_\xi z_\eta - z_\xi y_\eta$$

is termed the Jacobian of the transformation from y, z to ξ, η.

By differentiation of equations (B1) to (B3) and subsequent simplification, equations (B5) and (B6) lead to

$$\phi_\theta = -\frac{1}{4} \frac{\omega(a + b)^2 c^2 e^{-2\xi}\left(\sin^2 2\eta - \sinh 2\xi \cos 2\eta\right)}{J} \tag{B7}$$

and

$$\phi_y{}^2 + \phi_z{}^2 = \frac{1}{4}\frac{\omega^2(a + b)^4 e^{-4\xi}}{J} \tag{B8}$$

The substitution of equations (B7) and (B8) in equation (B4) gives the excess pressure as

$$\Delta P = \frac{\rho \omega^2 (a + b)^2}{8} \frac{2c^2 e^{-2\xi} \left(\sin^2 2\eta - \sinh 2\xi \cos 2\eta \right) - (a + b)^2 e^{-4\xi}}{J} \quad \text{(B9)}$$

The excess pressure force on an element of surface of the elliptic cylinder of unit length in the axial direction (x-direction) has a component parallel to the y-axis of amount

$$dF = -\Delta P_{\xi = \xi_0} \, dz$$

At the surface of the cylinder $\left(\xi = \xi_0 \right)$,

$$\left.\begin{array}{c} y = c \cosh \xi_0 \cos \eta = a \cos \eta \\[2ex] z = c \sinh \xi_0 \sin \eta = b \sin \eta \end{array}\right\} \quad \text{(B10)}$$

Therefore

$$dF = -\Delta P_{\xi = \xi_0} \, b \cos \eta \, d\eta \quad \text{(B11)}$$

Substituting equation (B9) into equation (B11) with $\xi = \xi_0$, eliminating ξ_0 and c by means of equations (B10), and evaluating J gives

$$dF = - \frac{\rho \omega^2 (a + b)^2 \left[2(a - b)^2 \left(\sin^2 2\eta - \frac{2ab}{a^2 - b^2} \cos 2\eta \right) - (a - b)^2 \right] b \cos \eta \, d\eta}{8 \left(a^2 \sin^2 \eta + b^2 \cos^2 \eta \right)}$$

$$\text{(B12)}$$

For $b \ll a \left(\xi_0 \ll 1 \right)$ this is approximately

$$dF = -\frac{\rho \omega^2 a^4 b \left(2 \sin^2 2\eta - 1 \right) \cos \eta \; d\eta}{8 \left(a^2 \sin^2 \eta + b^2 \right)}$$

The integral from the middle of the bottom surface around the right edge to the middle of the top surface is

$$Y = \int_{\eta=-\frac{\pi}{2}}^{\frac{\pi}{2}} dF$$

and

$$\lim_{\frac{b}{a} \to 0} Y = \frac{\pi}{8} \rho \omega^2 a^3 \tag{B13}$$

This gives the suction per unit length acting at the edges of a rotating flat plate of semiwidth a.

APPENDIX C

INTEGRATION OF PRESSURE FIELD OVER PLANE NORMAL TO AXIS

OF WAKE OF UNTWISTED PROPELLER

For purposes of calculation the flat-ribbon wake may be considered the limiting form of an elliptic cylinder as the minor axis shrinks to zero. Thus, the excess of the local pressure over the stream pressure derived in appendix B is applicable likewise here.

In any plane x = Constant, an element of area in the coordinates ξ, η is given by $J\,d\xi\,d\eta$ where J is the Jacobian defined after equation (B6). The excess pressure force on this element of area is

$$dF = \Delta P J\,d\xi\,d\eta$$

Substituting for ΔP from equation (B9) gives

$$dF = \frac{\rho\omega^2(a+b)^2}{8}\left[2c^2 e^{-2\xi}\left(\sin^2 2\eta - \sinh 2\xi\,\cos 2\eta\right) - (a+b)^2 e^{-4\xi}\right]d\xi\,d\eta$$

$$= \frac{\rho\omega^2(a+b)^2}{8}\left\{c^2\left[2e^{-2\xi}\sin^2 2\eta + \left(e^{-4\xi} - 1\right)\cos 2\eta\right] - (a+b)^2 e^{-4\xi}\right\}d\xi\,d\eta$$

$$(C1)$$

The excess pressure force on the entire plane x = Constant is obtained by integrating from 0 to 2π in η and from ξ_0 to ∞ in ξ, where $\xi = \xi_0$ defines the boundary of the elliptic cylinder. The integration gives

$$F = \frac{\pi}{8}\rho\omega^2(a+b)^2\left[e^{-2\xi_0}c^2 - \frac{1}{2}e^{-4\xi_0}(a+b)^2\right]\qquad(C2)$$

The limit of this expression as the elliptic cylinder shrinks into a flat ribbon $\left(\dfrac{b}{a} \longrightarrow 0, \quad \xi_0 \longrightarrow 0, \quad c \longrightarrow a\right)$ is

$$\lim_{\frac{b}{a} \to 0} F = \frac{\pi}{16}\rho\omega^2 a^4$$

Since the semiwidth a of the flat-ribbon wake is one-half the diameter D of the triangle; this is

$$F = \frac{\pi}{256}\rho\omega^2 D^4 \tag{C3}$$

which is in agreement with equation (7).

APPENDIX D

COMPONENT OF RESULTANT VELOCITY NORMAL TO LEADING EDGE

OF TWISTED TRIANGLE IN SCREW MOTION

The twisted triangle may be defined within its envelope cone

$$r = c_1 x \qquad (D1)$$

by the screw surface

$$\theta = c_2 x \qquad , \qquad (D2)$$

An element of the edge may be expressed by

$$d\bar{s} = \bar{r}_1 \, dr + \bar{\theta}_1 r \, d\theta + \bar{1} \, dx$$

where $\bar{r}_1$ is a unit vector in the direction of increasing r, $\bar{\theta}_1$ is a unit vector in the direction of increasing θ, and $\bar{1}$ is a unit vector along x. Thus

$$\frac{d\bar{s}}{dx} = \bar{r}_1 \frac{dr}{dx} + \bar{\theta}_1 r \frac{d\theta}{dx} + \bar{1}$$

$$= \bar{r}_1 c_1 + \bar{\theta}_1 r c_2 + \bar{1} \qquad (D3)$$

by equations (D1) and (D2).

Let $\bar{n}$ be a vector lying in the surface and perpendicular to the edge with positive sense outward. It may be obtained by the triple vector product

$$\bar{n} = \frac{d\bar{s}}{dx} \times \left(\bar{r}_1 \times \frac{d\bar{s}}{dx} \right)$$

$$= \left(\frac{ds}{dx} \right)^2 \bar{r}_1 - \left(\frac{d\bar{s}}{dx} \cdot \bar{r}_1 \right) \frac{d\bar{s}}{dx}$$

$$= \left(\frac{ds}{dx} \right)^2 \bar{r}_1 - c_1 \frac{d\bar{s}}{dx}$$

$$= \left(1 + c_2{}^2 r^2 \right) \bar{r}_1 - c_1 c_2 r \bar{\theta}_1 - c_1 \bar{i} \qquad (D4)$$

Compounding the axial and rotational velocities gives the resultant velocity

$$\bar{V}_R = V\bar{i} + \omega r \bar{\theta}_1 \qquad (D5)$$

The velocity component normal to the leading edge of the triangle is the negative of the component of the resultant velocity along $\bar{n}$

$$V_n = \frac{-\bar{V}_R \cdot \bar{n}}{|n|}$$

$$= \frac{c_1 V + c_1 c_2 \omega r^2}{\sqrt{c_1{}^2 \left(1 + c_2{}^2 r^2 \right) + \left(1 + c_2{}^2 r^2 \right)^2}}$$

whence

$$\left(\frac{V}{V_n} \right)^2 = \frac{c_1{}^2 \left(1 + c_2{}^2 r^2 \right) + \left(1 + c_2{}^2 r^2 \right)^2}{c_1{}^2 \left(1 + \frac{c_2 \omega r^2}{V} \right)^2} \qquad (D6)$$

At this point, c_1 may be identified with the tangent of the semi-vertex angle dr/dx and c_2, with the expression $2\pi/p$ where p is the pitch.

The assumption of the windmilling condition (zero local angle of attack) simplifies the expression with little loss in accuracy for other conditions. This condition is specified by putting $c_2 = \frac{\omega}{V}$, which is equivalent to $J = \frac{p}{D}$, and gives

$$\left(\frac{V}{V_n}\right)^2 = \frac{c_1^2\left(1 + \frac{\omega^2 r^2}{V^2}\right) + \left(1 + \frac{\omega^2 r^2}{V^2}\right)^2}{c_1^2\left(1 + \frac{\omega^2 r^2}{V^2}\right)^2}$$

$$= \frac{1}{1 + \frac{\omega^2 r^2}{V^2}} + \frac{1}{c_1^2} \tag{D7}$$

But from equation (D1), $\frac{1}{c_1} = \frac{dx}{dr}$, and from equation (D5)

$$\left(\frac{V}{V_R}\right)^2 = \frac{1}{1 + \frac{\omega^2 r^2}{V^2}} \tag{D8}$$

Therefore, equation (D7) may be written

$$\left(\frac{V}{V_n}\right)^2 = \left(\frac{V}{V_R}\right)^2 + \left(\frac{dx}{dr}\right)^2 \tag{D9}$$

Equation (D9) relates the velocity component normal to the leading
odge V_n to the stream velocity V, the resultant of the stream
and rotational velocities V_R, and the reciprocal dx/dr of the
slope of the envelope cone of the twisted triangle.

The equation is still valid if equation (D1) is replaced by

$$r = f(x)$$

and c_1 is interpreted as the local value of dr/dx, which is now
a function of x. This generalizes the triangle into the flatiron
and other shapes. Suppose it is desired to maintain a constant
normal velocity component V_n all along the leading edge. A
variable sweepback or flatiron plan form is required. Equation (D9)
together with equation (D8) may be interpreted as the differential
equation in r and x that specifies the necessary plan form.

REFERENCES

1. Jones, Robert T.: Properties of Low-Aspect-Ratio Pointed Wings
     at Speeds below and above the Speed of Sound. NACA TN No. 1032,
     1946.

2. Puckett, Allen E.: Supersonic Wave Drag of Thin Airfoils. Jour.
     Aero. Sci., vol. 13, no. 9, Sept. 1946, pp. 475-484.

3. Lamb, Horace: Hydrodynamics. Reprint of sixth ed. (first American
     ed.), Dover Publications (New York), 1945, pp. 86-88.

4. Betz, Albert: Screw Propellers with Minimum Energy Loss. R.T.P.
     Translation No. 43, British Ministry of Aircraft Production.

5. Cohen, Doris: A Method for Determining the Camber and Twist of
     a Surface to Support a Given Distribution of Lift. NACA TN
     No. 855, 1942.

TABLE I - CALCULATION OF PLAN FORM FOR PROPELLER OF EXAMPLE

Row	Item	Value						Explanation
(1)	r, ft	0	1.5	3.0	4.5	5.5	6.0	Radius
(2)	$\left(v_R/v\right)^2$	1.000	1.051	1.202	1.456	1.681	1.810	$\left(\dfrac{\text{Resultant velocity}}{\text{Stream velocity}}\right)^2;\quad 1 + \dfrac{\pi^2}{J^2}\dfrac{r^2}{R^2}$
(3)	$\dfrac{dx}{dr}$	1.000	1.024	1.080	1.146	1.185	1.203	$\sqrt{\left(\dfrac{v}{v_n}\right)^2 - \left(\dfrac{v}{v_R}\right)^2}\quad\text{with}\quad \dfrac{v}{v_n} = \sqrt{2}$
(4)	x, ft	0	1.52	3.10	4.77	5.90	6.53	Graphical integration
(5)	Projected blade chord	6.53	5.01	3.43	1.76	[a]0.90	[a]0	$\dfrac{v}{v_R} \times$ Blade chord; $6.53 - (4)$
(6)	$\left(v_R/v\right)^4$	1.000	1.105	1.446	2.120	2.828	3.277	$(2)^2$
(7)	b_{wt}, ft	6.53	5.54	4.97	3.73	2.545	0	$\left(\dfrac{v_R}{v}\right)^3 \times$ Blade chord; $(5) \times (6)$

$$S_{wt} = \int_{-R}^{R} b_{wt}\ dy = 55.2\ \text{ft}^2$$

[a]Plan form of this example (fig. 10) deviates from curve of r against x defined by rows (1) and (4) beyond $r = 5.5$ in order to provide tip fairings.

NATIONAL ADVISORY
COMMITTEE FOR AERONAUTICS

TABLE II - CALCULATION OF PERFORMANCE FOR PROPELLER OF EXAMPLE

$$\left[M = 1.1\right]$$

(1)	(2)	(3)	(4)	(5)	(6)	(7)
J	p/D	Skin-friction drag coefficient, C_{D_f}	Pressure drag coefficient, C_{D_p}	C_D	$C_D S_{wt}$	Ideal efficiency, η_i (percent)
Specified	Specified	Estimated	Estimated from reference 2	$C_{D_f} + C_{D_p}$	$55.2 C_D$	$\frac{1}{2}\left(1 + \frac{J}{p/D}\right)100$
3.49	4.37	0.0046	0.0037	0.0083	0.458	90.0

(8)	(9)	(10)	(11)	(12)	(13)	(14)
True airspeed (mph)	Profile drag (lb)	ω (radians/sec)	Ideal thrust, T_i (lb)	Net thrust, T (lb)	Brake-horsepower, bhp	Net efficiency η (percent)
	$(6) \times \frac{1}{2}\rho V^2$	$2\pi V/JD$	From equation (15)	T_i - Profile drag	$\frac{\omega}{550}\left[\frac{1}{256}\rho\omega^2 D^5 J\left(1 - \frac{J}{p/D}\right)\right]$	$TV/5.5\text{bhp}$
Sea level						
837	820	184.2	7440	6620	18,460	80.0
Altitude of 25,000 ft (density ratio = 0.45)						
761	305	167.5	2765	2460	6,240	80.0

NATIONAL ADVISORY
COMMITTEE FOR AERONAUTICS

Fig. 1

Mach cone;
M = 2

Plan view

Side view
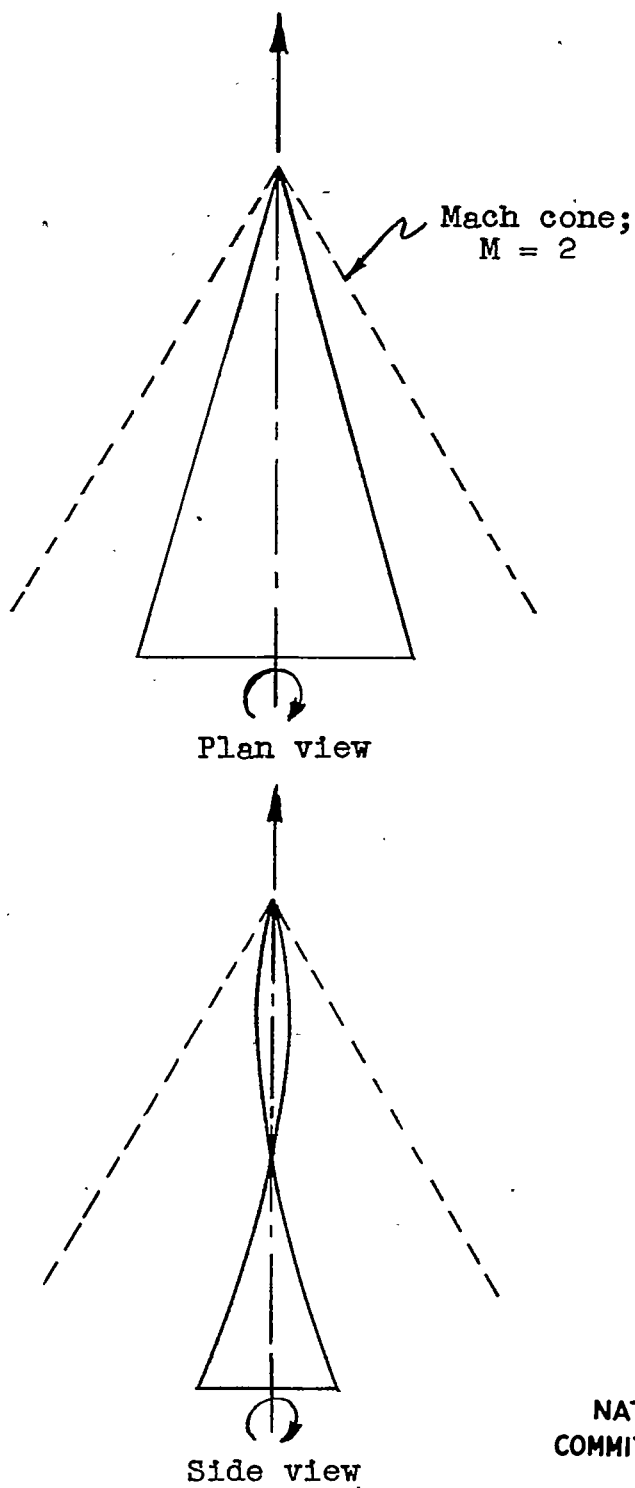
NATIONAL ADVISORY
COMMITTEE FOR AERONAUTICS

Figure 1.— Transonic propeller of triangular plan form.
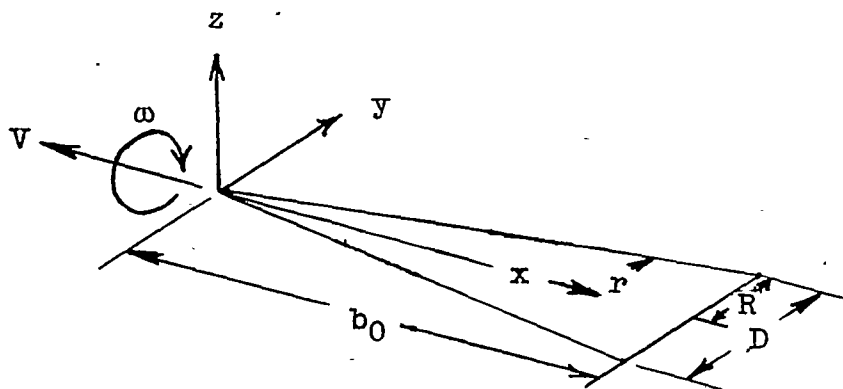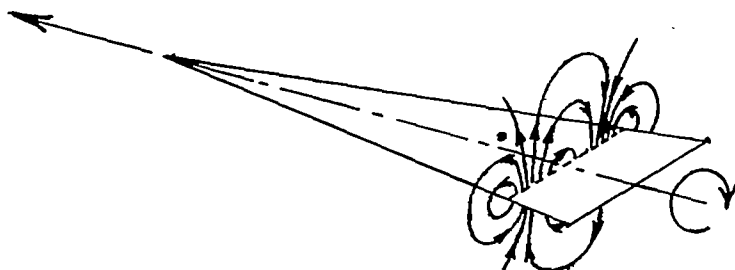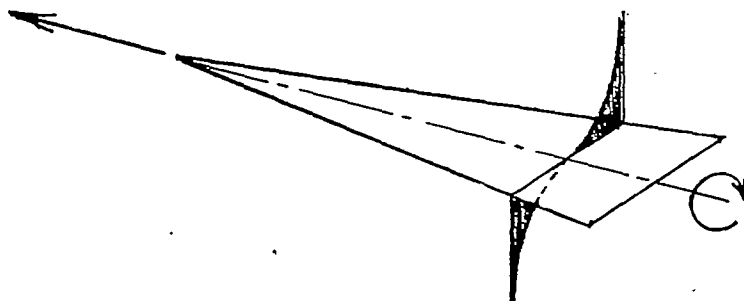
Figure 2.— Coordinate system and notation.

Figure 3.— Flow pattern.

NATIONAL ADVISORY
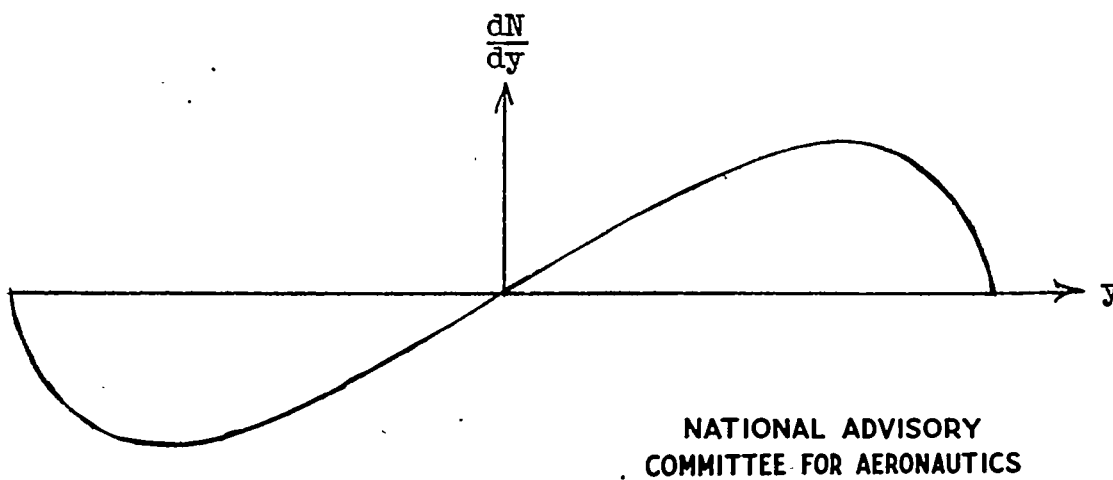COMMITTEE FOR AERONAUTICS

Figure 4.— Pressure distribution.

$$\frac{dN}{dy}$$

NATIONAL ADVISORY
COMMITTEE FOR AERONAUTICS

Figure 5.— Distribution of normal force along span.

NATIONAL ADVISORY
COMMITTEE FOR AERONAUTICS
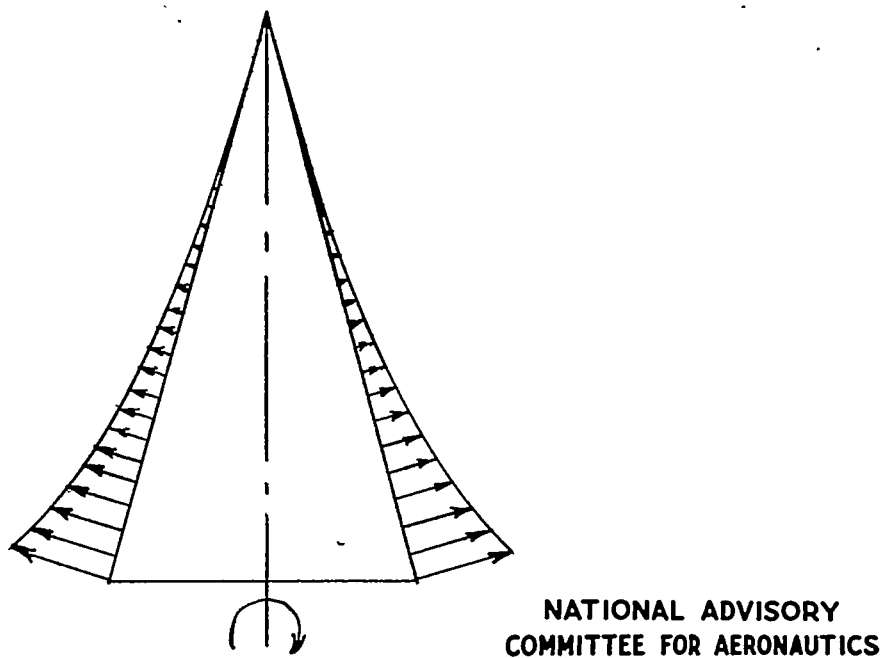
Figure 6.— Suction along leading edges.
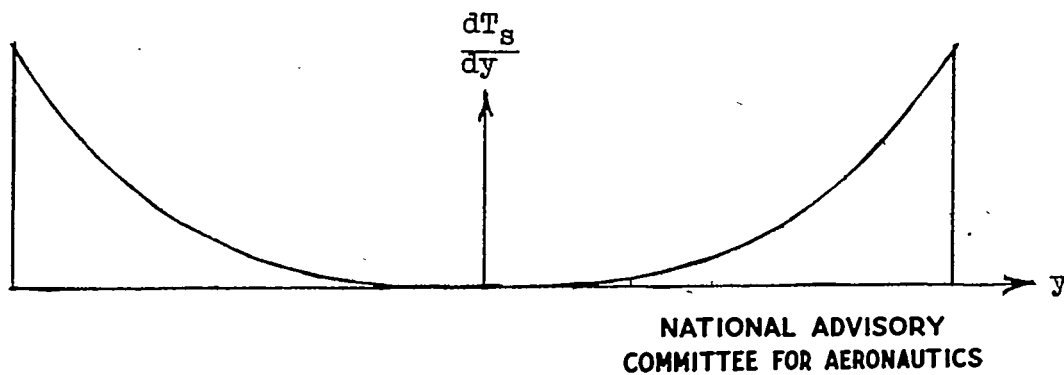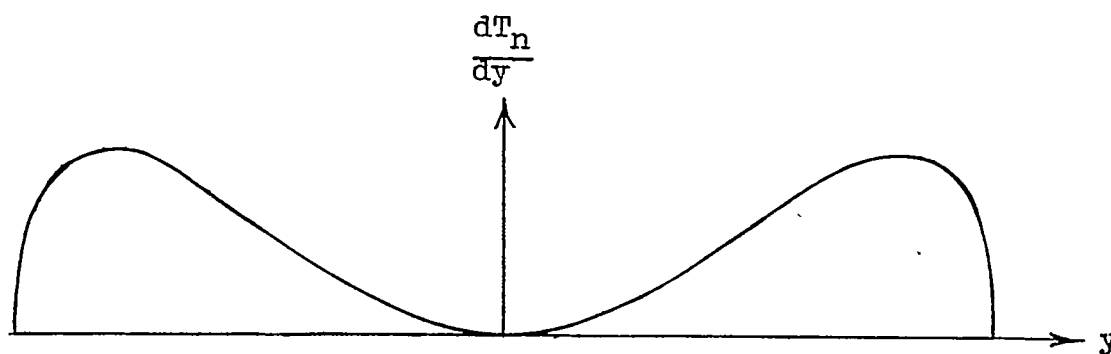
Figure 7.— Distribution of suction thrust along span.
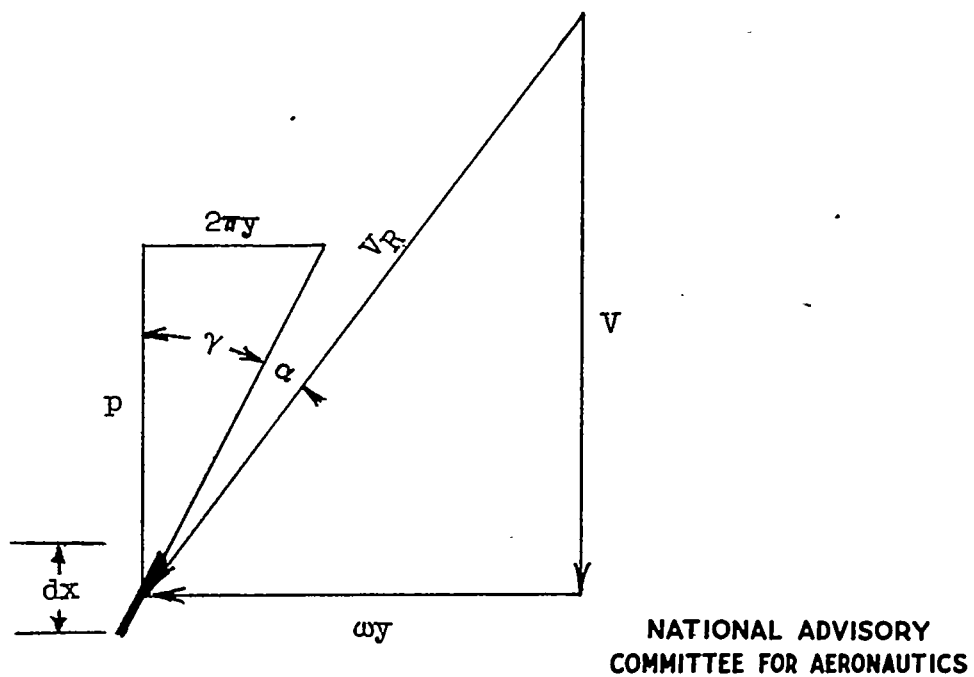
Figure 8.— Attitude γ and angle of attack α of a
blade element at radius y.

Figure 9.— Distribution of thrust component of normal force along span.

Fig. 10
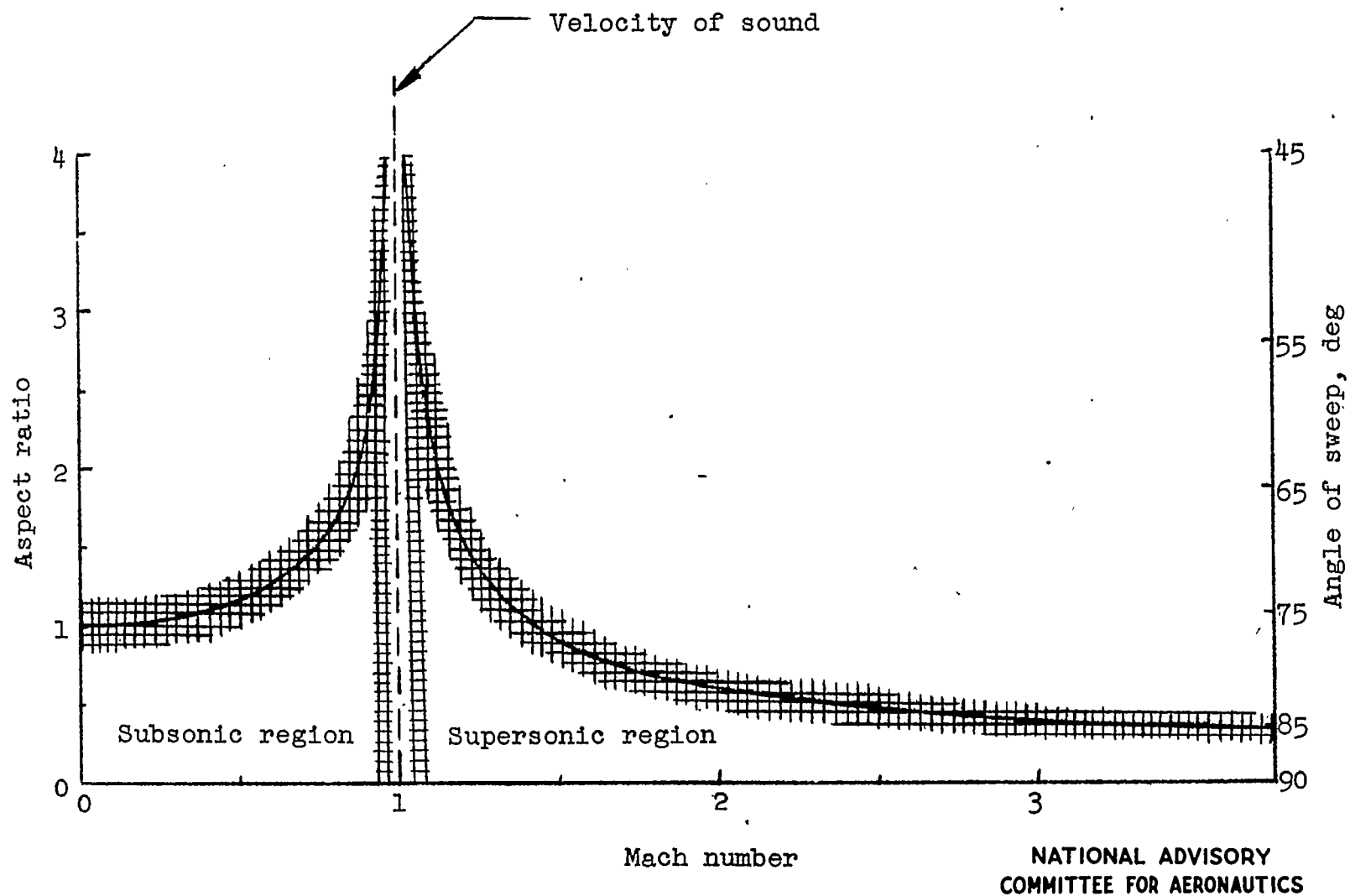
Figure 10.— Regions in which theory of two–dimensional flows is good approximation.
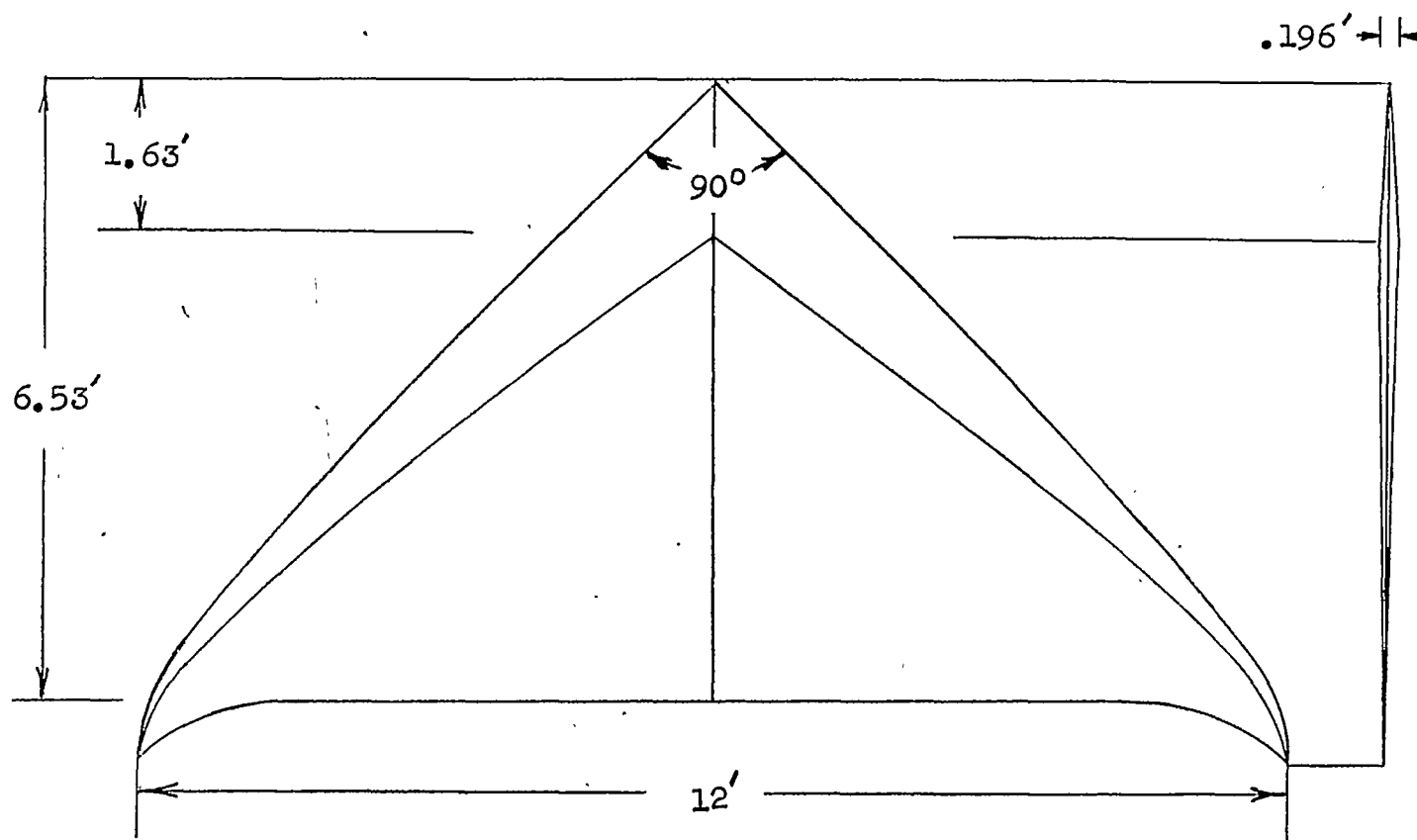
Figure 11.— Propeller design for Mach number 1.1 arrived at in example. For simplicity, the twist is not shown. (Double-wedge section is chosen for purposes of computation only and is not recommended in practice.)

Fig. 11